AD-A247 660

UMENTATION PAGE

Form Approved
OBM No. 0704-0188

2. Report Date.	3. Report Type and Dates Covered.
November 1991	Final - Journal Article

4. Title and Subtitle.
Three-dimensional angular distributions of acoustic scattering from flexural and Rayleigh resonances of elastic spheroidal targets

5. Funding Numbers.

Contract	
Program Element No.	0601153N
Project No.	03202
Task No.	360
Accession No	DN257033
Work Unit No.	12211C

6. Author(s).
Jacob George and M. F. Werby

7. Performing Organization Name(s) and Address(es).
Naval Oceanographic and Atmospheric Research Laboratory
Ocean Acoutics and Technology Directorate
Stennis Space Center, MS 39529-5004

8. Performing Organization Report Number.
JA 221:051:91

9. Sponsoring/Monitoring Agency Name(s) and Address(es).
Naval Oceanographic and Atmospheric Research Laboratory
Basic Research Management Office
Stennis Space Center, MS 39529-5004

10. Sponsoring/Monitoring Agency Report Number.
JA 221:051:91

11. Supplementary Notes.

12a. Distribution/Availability Statement.
Approved for public release; distribution is unlimited.

12b. Distribution Code.

13. Abstract *(Maximum 200 words).*
Three-dimensional angular distributions of acoustic scattering strength arising from flexural and Rayleigh resonances of a prolate steel spheroid are presented. Flexural resonances are found to produce strong scattering into four almost symmetrical lobes, by as much as 20 dB above the nonresonant background. Rayleigh resonances are weaker, but significant portions of the scattered Rayleigh energy are radiated into steep angles. In both cases, considerable interactions of the scattered energy with waveguide boundaries may be expected.

14. Subject Terms.
Acoustic waves, elastic waves, seismic waves

15. Number of Pages.
4

16. Price Code.

17. Security Classification of Report.	18. Security Classification of This Page.	19. Security Classification of Abstract.	20. Limitation of Abstract.
Unclassified	Unclassified	Unclassified	SAR

Three-dimensional angular distributions of acoustic scattering from flexural and Rayleigh resonances of elastic spheroidal targets

Jacob George and M. F. Werby
Naval Oceanographic and Atmospheric Research Laboratory, Code 221, Stennis Space Center, Mississippi 39529

(Received 23 May 1991; accepted for publication 25 July 1991)

Three-dimensional angular distributions of acoustic scattering strength arising from flexural and Rayleigh resonances of a prolate steel spheroid are presented. Flexural resonances are found to produce strong scattering into four almost symmetrical lobes, by as much as 20 dB above the nonresonant background. Rayleigh resonances are weaker, but significant portions of the scattered Rayleigh energy are radiated into steep angles. In both cases, considerable interactions of the scattered energy with waveguide boundaries may be expected.

PACS numbers: 43.30.Gv, 43.20.Fn

INTRODUCTION

While resonances of submerged elastic objects such as spheres and infinite cylinders have been studied over the past several decades, resonances of the more complicated targets such as spheroids and finite cylinders have been investigated only recently. For spheres and cylinders, it has long been known[1] that the resonances can be labeled by an index pair (n,l) where n is the mode order in the normal-mode series solution for the scattered field, and l labels each individual resonance within each mode n. The family of resonances identified by $l=1$ is called the Rayleigh family,[1] and families labeled by $l>1$ have been called Whispering Gallery resonances.[1,2] Echoes returned by elastic prolate spheroids also exhibit Rayleigh resonances[3,4] for aspect ratios as high as $L/D=10$, where L is the length and D the diameter. It was shown[4] that the frequency of a given resonance increased with the L/D ratio, and that resonance could be excited at any aspect angle.

In addition to the Rayleigh and Whispering Gallery resonances, other resonances having a flexural origin have been predicted recently for prolate elastic spheroids.[5] Unlike in the Rayleigh case, the frequency of these resonances decrease with increasing L/D ratio. Their amplitudes are about three times those of the Rayleigh resonances for equivalent spheres circumscribing the spheroids. The flexural origin was verified by comparing the resonance frequencies for spheroids predicted by the extended boundary condition (EBC) method,[6-13] with those of free-free Timoshenko beams[14-16] of circular cross sections possessing the same aspect ratios. The agreement is very good, and becomes better for increasing aspect ratios L/D.

In earlier work,[4,5] bistatic angular distributions were given in the plane defined by the incident signal (plane wave) and the major axis of the prolate spheroid. In the present paper, we study the three-dimensional angular distributions of scattering strength of both the flexural and the Rayleigh resonances for different incident angles. We present three-dimensional polar plots of scattering strength, giving additional insights into these resonances.

I. THE EXTENDED BOUNDARY CONDITION METHOD

Since detailed discussions of the EBC technique are available in the literature,[6-13] here we only present the formulas which facilitated easy computation of the three-dimensional scattering strength distributions. The T matrix relates the partial wave coefficients $\{f\}$ of the scattered field to the corresponding coefficients $\{a\}$ of the incident field through a matrix equation:

$$f = Ta,$$

where T is the T matrix. The T matrix is only a function of the boundary conditions and the shape of the object. Consequently, once T is known, the scattered field can be determined for any chosen incident field a. In our calculation, the incident signal is a plane wave.

The differential scattering cross section $d\sigma/d\Omega$ can be written in terms of the T matrix as

$$\frac{d\sigma}{d\Omega} = |f(\Omega)|^2,$$

$$f(\Omega) = \left(\frac{1}{4\pi}\right)^{1/2} \Sigma a_{lm} T^{m}_{ll'} Y_{lm}(\theta,\phi) Y^{*}_{l'm}(\theta',\phi'),$$

where the pair (θ,ϕ) denote the incident direction, (θ',ϕ') the scattering direction, and the sum runs over the partial waves l, l', and m. The Ys are spherical harmonics. The a_{lm} are the plane-wave expansion coefficients. The advantage of this formula is that once the T matrix is calculated, subsequent computations of the scattering cross section for an incident signal direction defined by (θ,ϕ) and a scattered signal direction defined by (θ',ϕ') can be done quickly through a few simple multiplications and additions.

II. THREE-DIMENSIONAL BEAM PATTERNS

We present scattering from a prolate solid elastic spheroid, with axial symmetry about its main axis. Its three-dimensional beam pattern (acoustic scattering strength as a function of spherical polar angles) may be visualized as a closed surface about the spheroid. This surface is such that

 0001-4966/91/112847-04$00.80

the radius vector from the center of the spheroid to any point on the beam pattern would be proportional to the scattering strength in the direction of the radius vector. We present the beam pattern as a wire-frame plot with three-dimensional perspective for easy visualization. To define the coordinate system, let us assume that the spheroid major axis is horizontal. Then the eye of the observer would be located in the vertical plane containing the axis, at approximately 65° elevation above the axis, far away from the spheroid. The incident signal (plane wave) would be in the horizontal plane. For end-on incidence, the line joining the eye to the center of the spheroid would subtend an acute angle of 65° with the incoming signal along the axis. For broadside incidence, the signal would be coming from the right of the observer.

For convenience of comparison, figures on a given frame are drawn on the same dB scale. This allows easy visualization of the build up and subsequent decay of a resonance as the frequency is varied from a point below the resonance to a point above it. The polar origin in each figure is chosen to be at approximately 30 dB below the maximum scattering strength value on a given frame.

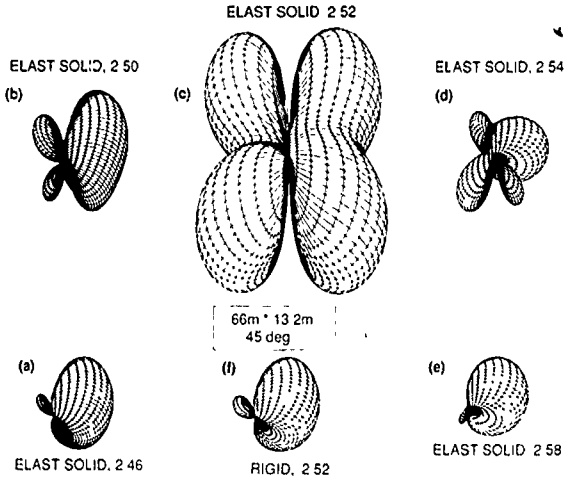

FIG. 2. The variation in the three-dimensional angular distribution of scattering strength as $kL/2$ is varied from a value below the flexural resonance point 2 52 (Fig 1) to a value above it [(a)–(e)]. The rigid scattering pattern is shown in (f) Incident angle is 45°.

A. Flexural resonances

We focus on the first two flexural resonances of the steel spheroid in water with aspect ratio $L/D = 5$ ($L = 66$ m, $D = 13.2$ m), reported in Ref. 5. These occur at $kL/2 = 2.52$ and 5.15, respectively, where k is the wave number. The material parameters used in the calculation are: for steel, density = 7700 kg/m^3, compressional speed = 5950 m/s, shear speed = 3240 m/s; for water, density = 1000 kg/m^3, compressional speed = 1482.5 m/s. Figure 1 shows the three-dimensional angular distributions of scattering strengths for the elastic spheroid at the first resonance ($kL/2 = 2.52$), compared with the corresponding rigid body distributions. Figure 1(a) and (d) for end-on incidence are nearly identical, indicating that the flexural resonance is not excited in this case. This is expected, considering that incidence along the axial direction does not favor any transverse vibrations. Figure 1(b) and (e) for 45° incidence show strong excitation of the flexural resonance with four almost symmetric lobes. Figure 1(c) and (f) for broadside incidence exhibit a weak excitation of the resonance.

Figure 2(a)–(e) for 45° incidence, address the same resonance as in Fig. 1, but illustrate the variation of the angular distribution pattern as $kL/2$ (and thus the frequency) is varied from a value below the resonance point to a value above it. It is clear that for a change of only 0.06 in $kL/2$ above or below its resonance value 2.52, the angular distribution pattern approaches that for a rigid body [Fig. 2(f)]. At resonance the flexural excitation is quite strong, with scattering

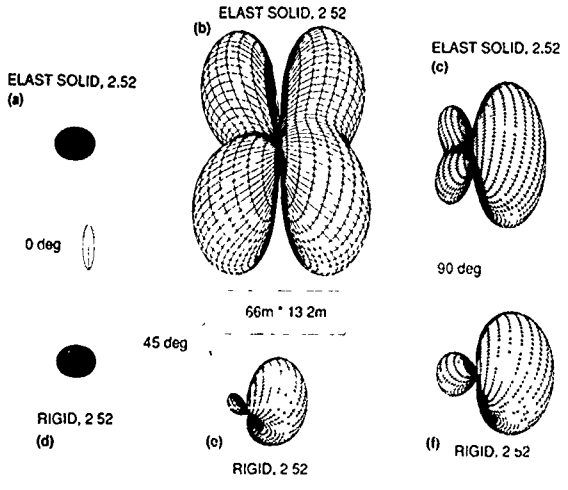

FIG. 1. Three-dimensional angular distributions of scattering strength at a flexural resonance ($kL/2 = 2.52$) for plane-waves incident on a prolate steel spheroid, compared with similar distributions for a rigid body of identical dimensions. Spheroid length is 66 m, and diameter 13.2 m (a) and (d) are for end-on incidence; (b) and (e) for 45° incidence; (c) and (f) for broadside incidence Coordinate system explained in Sec. II.

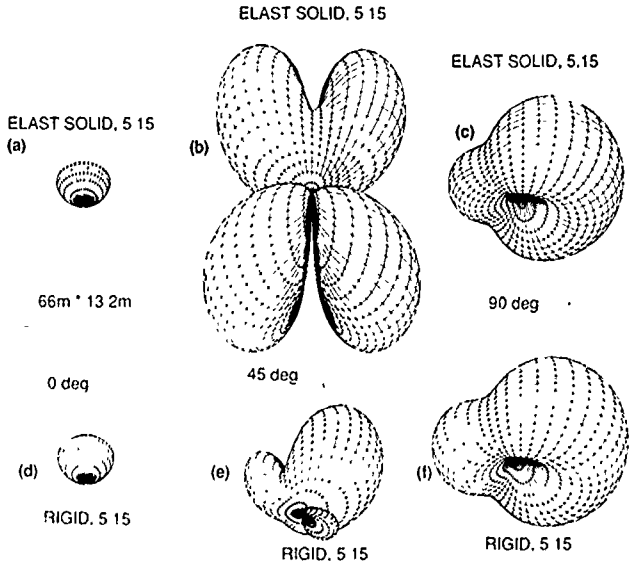

FIG 3. Similar to Fig 1, for flexural resonance at $kL/2 = 5.15$

strength greater than 20 dB above the nonresonant background.

Figure 3 is similar to Fig. 1, for the second flexural resonance at $kL/2 = 5.15$. Figure 4 is similar to Fig. 2, again for the second flexural resonance at $kL/2 = 5.15$. The features are similar for both resonances. But the second resonance is broader, as a change of 0.6 (instead of 0.06) in $kL/2$ is needed before the elastic target has a pattern closer to the rigid body case.

B. Rayleigh resonances

Here, we focus on the first Rayleigh resonance of the steel spheroid in water with aspect ratio $L/D = 4$ ($L = 66$ m, $D = 16.5$ m), reported in Ref. 4. This resonance occurs at $kL/2 = 7.4$. The material parameters used in the calculation are the same as in Sec. II A. The results are shown in Fig. 5 (arranged similar to Fig. 1), and in Fig. 6 (arranged similar to Fig. 2). In the present case, the strongest excitation of the Rayleigh resonance is for end-on incidence [Fig. 5(a) and (d)]. Incident signal at 45° [Fig. 5(b) and (e)], and at 90° [Fig. 5(c) and (f)] only weakly excite the Rayleigh mode about the largest meridian. Figure 6 shows that the resonance is comparable in width (in frequency domain) to the second flexural resonance discussed in Sec. II A. A change of 0.4 in $kL/2$ is needed to bring down the resonance closer to the rigid body case.

A notable feature of the Rayleigh resonance is the significant amount of scattered energy directed to very steep angles. This has important implications for applications to object in a waveguide, since substantial energy will be reflected from the top and bottom surfaces of the waveguide. This feature contrasts with the behavior of flexural resonances where very little energy is scattered into very steep angles.

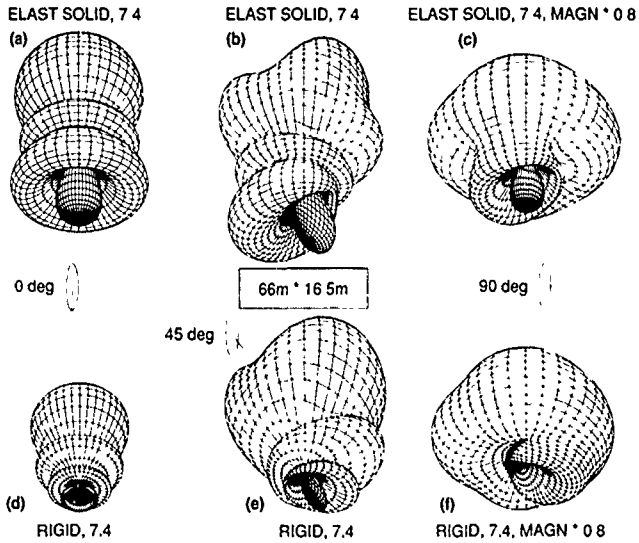

FIG 5 Similar to Fig. 1, for Rayleigh resonance at $kL/2 = 7.4$. Spheroid length is 66 m, and diameter 16.5 m.

III. CONCLUSIONS

Three-dimensional angular distributions of acoustic scattering strength arising from flexural and Rayleigh resonances of a prolate steel spheroid are presented. The flexural resonances are particularly significant because they are strongly excited by more than 20 dB above the nonresonant background, when the incident angle is between 35° and 55° relative to the axis of symmetry. We have found that at the flexural resonances, energy is scattered into four almost symmetric lobes, with most of the energy scattered into the

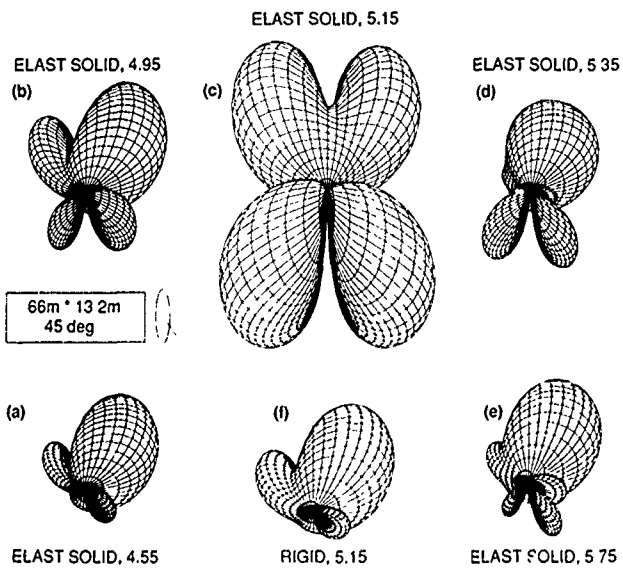

FIG. 4. Similar to Fig. 2, for flexural resonance at $kL/2 = 5.15$.

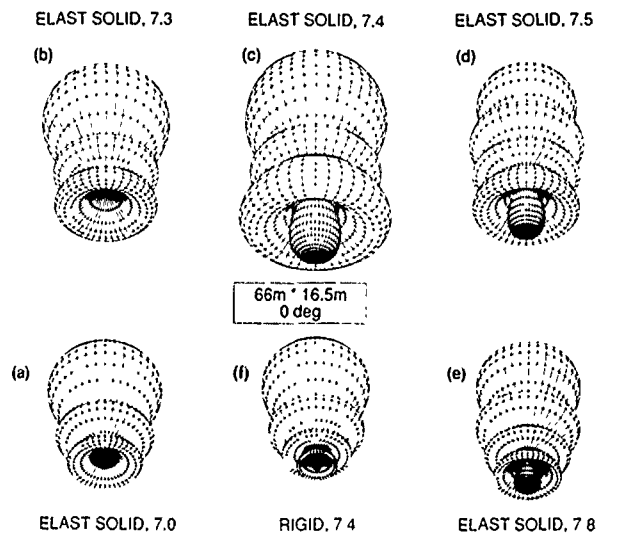

FIG. 6 Similar to Fig 2, for Rayleigh resonance at $kL/2 = 7.4$. Spheroid length is 66 m, and diameter 16 5 m. End-on incidence.

horizontal plane. However, much energy is radiated above and below the horizon so that flexural modes will cause significant interaction with waveguide boundaries. In contrast, Rayleigh resonances are weaker, but major portions of the scattered Rayleigh energy are directed into steep angles. This too can cause considerable interaction with waveguide boundaries.

ACKNOWLEDGMENTS

Financial support for this work was provided by NOARL program element 0601135N (Program Manager: Halcyon Morris). The computations were done on the VAX8650 computer at NOARL.

[1]L Flax, L R Dragonette, and H. Uberall, "Theory of elastic resonance excitation by sound scattering," J. Acoust. Soc. Am. **63**, 723 (1978) (1975); also Lord Rayleigh, Philos. Mag **5**, 458 (1877).
[2]Lord Rayleigh, Philos. Mag. **5**, 458 (1877).
[3]M. Werby and G. Tango, "Numerical study of material properties of submerged elastic objects using resonance responses," J. Acoust Soc Am. **79**, 1260–1269 (1986).
[4]M. F. Werby and G. C Gaunaurd, "Resonance scattering from submerged elastic spheroids of high aspect ratios and its three-dimensional interpretation," J. Acoust. Soc. Am **88**, 951–960 (1990).
[5]M. F. Werby and G C Gaunaurd, "Flexural resonances in obliquely insonified solid elastic spheroids," J. Acoust. Soc. Am. **85**, 2365–2371 (1989)
[6]P. C. Waterman, "New foundation of acoustic scattering," J. Acoust. Soc. Am. **45**, 1417 (1969).
[7]P C Waterman, "Matrix theory of elastic wave scattering," J Acoust Soc. Am. **60**, 567 (1976).
[8]*Acoustic, Electromagnetic, and Elastic Wave Scattering—Focus on the T-matrix Approach*, edited by V. K. Varadan and V. V. Varadan (Pergamon, New York, 1980).
[9]A. Bostrom, "Scattering of stationary acoustic waves by an elastic obstacle immersed in a fluid," J. Acoust. Soc. Am. **67**, 390 (1980).
[10]M. F. Werby and R D Evans, "Scattering from unbounded and bounded objects," IEEE J Ocean Eng. **OE-12**, 380 (1987)
[11]M. F Werby, "Application of the extended boundary condition equations to scattering from fluid-loaded bounded objects," Eng. Analysis **5**, 12 (1988).
[12]P. M. Morse and H. Feshbach, *Methods of Theoretical Physics* (McGraw-Hill, New York, 1953), Chap. 7.
[13]Y. H Pao and V V Varatharajulu, "Huygens' principle, radiation condition, and integral formula for scattering of elastic waves," J. Acoust. Soc. Am. **60**, 1361 (1976).
[14]S. P. Timoshenko, "On the correction for shear of the differential equation for transverse vibrations of prismatic bars," Philos. Mag. **41**, 744–746 (1921).
[15]S. P. Timoshenko, "On the transverse vibration of beams of uniform cross section," Philos. Mag. **43**, 125–131 (1922).
[16]B. Abbas and J. Thomas, "The second frequency spectrum of Timoshenko beams," J Sound Vib. **51**, 123–137 (1977).